Am J Nucl Med Mol Imaging 2018;8(6):428-440
www.ajnmmi.us /ISSN:2160-8407/ajnmmi0088184

Review Article

Preclinical PET tracers for the evaluation of sarcomas: understanding tumor biology

Ian R Sigal[1], Ronnie Sebro[1,2,3,4]

Departments of [1]Radiology, [2]Orthopedic Surgery, [3]Genetics, [4]Epidemiology and Biostatistics, University of Pennsylvania, 3400 Spruce Street, Philadelphia, PA 19104, USA

Received November 9, 2018; Accepted December 5, 2018; Epub December 20, 2018; Published December 30, 2018

Abstract: Sarcomas are rare tumors of mesenchymal origin. Sarcomas display significant histological heterogeneity, resulting in significant imaging heterogeneity. ^{18}F-FDG PET has is increasingly used for the evaluation, staging and surveillance of patients with sarcomas. ^{18}F-FDG PET maximum SUV has been shown to be correlated with sarcoma grade and overall survival. This has led to interest in alternative PET tracers to assess the biological characteristics of tumors and guide treatment decisions. Here we investigate novel PET/CT tracers used for the evaluation of sarcomas over the past 20 years and summarize what we have learned about sarcoma tumor biology from these studies.

Keywords: PET, sarcoma, amino acid PET tracers, nucleoside PET tracers, hypoxia imaging

Introduction

Bone and soft tissue sarcomas are a heterogeneous group of tumors thought to be derived from mesenchymal tissues [1]. Sarcomas are rare cancers which comprise approximately 21% of pediatric cancers and 1% of new cancer diagnoses in adults [1, 2]. The prognosis for sarcoma patients can vary dramatically. Five-year survival after a new sarcoma diagnosis in patients without metastatic disease is 65% [1], but varies due to many factors including histologic grade, sarcoma subtype, and tumor size [2-4]. Tumor type, size and histologic grade are among the most important prognostic factors for patients with sarcoma. Tumor grade is related to many histopathologic factors including mitotic activity, intra-tumoral necrosis, and tumor cell differentiation [5].

Imaging is essential for the evaluation and treatment of sarcoma. Magnetic resonance imaging (MRI) has been shown to be the best modality to assess tumor size, extent and neurovascular involvement for surgical and radiation therapy planning [6]. Computerized tomography (CT) is the best imaging modality for the detection of pulmonary metastases and used for staging [6]. There has been progressive increasing interest in metabolic and functional imaging of sarcomas. ^{18}F-Fluorodeoxyglucose (^{18}F-FDG) is a glucose analog which is taken up rapidly by tumor cells. This allows for identification of tumor cells with high glucose metabolism. ^{18}F-FDG positron emission tomography/computed tomography (PET/CT) is frequently utilized for sarcoma staging, surveillance, and to aid in biopsy guidance [1]. The maximum standardized uptake value (SUV) on ^{18}F-FDG PET/CT studies has been correlated with sarcoma grade [7-9] and overall survival [10-12]. ^{18}F-FDG PET/CT has also been shown to be clinically useful for differentiating benign from malignant peripheral nerve sheath tumors [13]. More recent reports suggest that ^{18}F-FDG PET/CT may also clinically differentiate enchondromas from chondrosarcomas [14]. The significant clinical success of ^{18}F-FDG PET/CT has resulted in significant interest in developing other PET tracers that can assist in the evaluation and treatment of patients with sarcoma.

Alternative PET/CT tracers are now being developed to take advantage of non-glucose metabolites to reveal information about sarcoma tumor biology that may have diagnostic or prognostic implications. Consequently, many PET/CT tracers are currently in development and

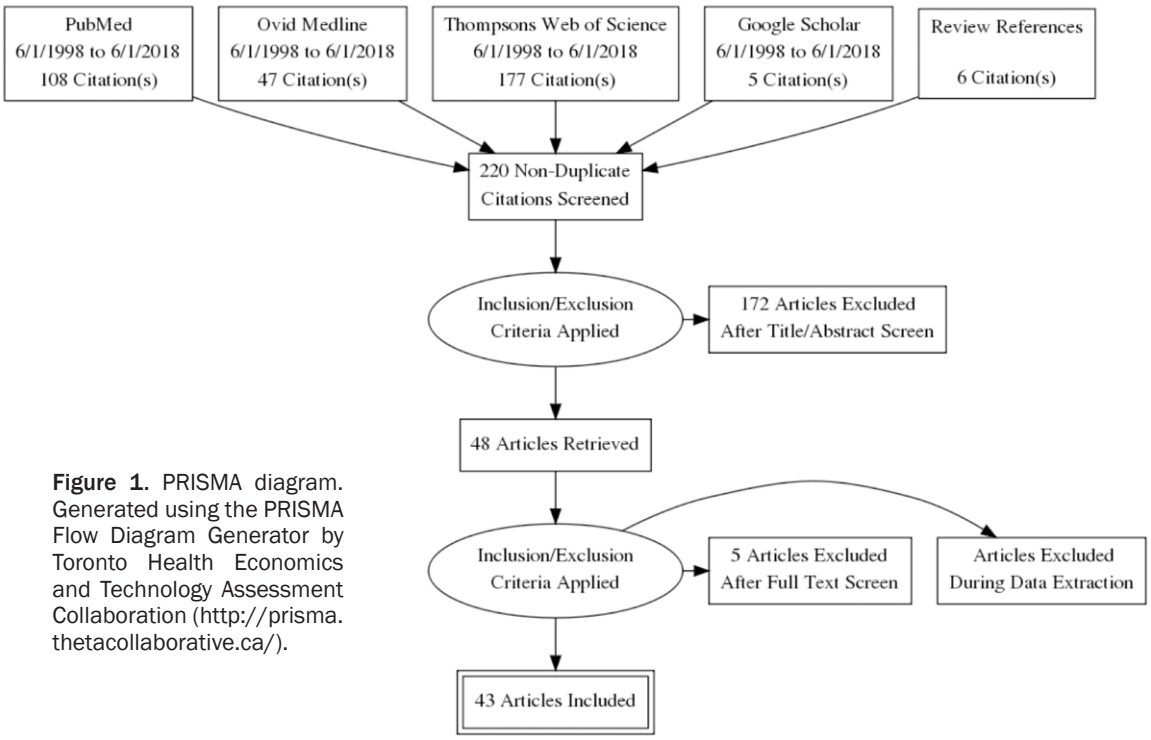

Figure 1. PRISMA diagram. Generated using the PRISMA Flow Diagram Generator by Toronto Health Economics and Technology Assessment Collaboration (http://prisma.thetacollaborative.ca/).

have been studied in the context of bone and soft tissue sarcoma. The purpose of this review is to identify preclinical PET/CT tracers that may be used in future for sarcoma imaging, and to evaluate what we have learned from using these tracers.

Literature search

Articles were identified to be included this review by searching in PubMed for "('positron emission' OR PET) AND (sarcoma) AND ([TRACER])". Analogous searches were performed using Google Scholar, Ovid Medline, and Thomson's Web of Science. Only articles written in English were assessed and only new PET tracers used between 01/01/2000 and 06/01/2018 were included. Studies with human subjects were included based on relevance to sarcoma clinical practice. **Figure 1** shows PRISMA diagram of how studies were selected for the review. **Table 1** shows novel PET tracer clinical characteristics.

Nucleoside analogues

^{11}C-thymidine

^{11}C-thymidine is a nucleoside analogue which is taken up and directly incorporated into the DNA of cancer cells [15]. ^{11}C-thymidine has a half-life of 20.4 minutes [16, 17], and the metabolic product $^{11}CO_2$ is excreted through exhalation [18]. ^{11}C-thymidine avidity is a direct measure of tumor cell DNA synthesis because it is incorporated into DNA [15]. This allows this PET tracer to assess how treatment including chemoradiation affects tumor DNA synthesis [15] and to differentiate tumor from non-replicative inflammatory cells [15]. ^{11}C-thymidine has been investigated as a component of multiagent PET to estimate sarcoma grade. In a small pilot trial, 10 patients with soft tissue sarcoma (STS) were imaged with ^{11}C-thymidine to visualize cellular proliferation, and these results were compared with histological grade [19]. No correlation was found between ^{11}C-thymidine avidity and sarcoma grade; however, thymidine flux values ranged from 0.0001 to 0.147 in different sarcoma types [19]. This suggests variation in sarcoma cellular proliferation between different sarcomas, which may have implications in treatment [19]. To assess the potential of ^{11}C-thymidine to measure tumor response to therapy, Shields et al. imaged two patients with high grade sarcoma before and after the initiation of chemotherapy using ^{18}F-FDG PET and ^{11}C-thymidine PET [15]. In one sarcoma patient, the steady state thymidine incorporation flux

Table 1. Characteristics of PET tracers for sarcoma imaging

Tracer	Analogue	Half-life	Clinical role
^{11}C-thymidine	Nucleic acid (thymidine)	20.4 minutes	Superior tumor-to-inflammation ratio
^{18}F-FLT	Nucleic acid (thymidine)	110 minutes	Estimation of tumor proliferation, grade, mitotic index, and response to therapy
^{11}C-methionine	Amino acid (methionine)	20.4 minutes	Superior tumor-to-inflammation ratio, estimation of response to therapy
^{18}F-FPMET	Amino acid (methionine)	110 minutes	Superior tumor-to-inflammation ratio
^{18}F-FPro	Amino acid (proline)	110 minutes	Accumulates in osteosarcoma in an animal model
^{11}C-tyrosine	Amino Acid (tyrosine)	20.4 minutes	Superior tumor-to-inflammation ratio, estimation of tumor PSR, grade, and mitotic index
^{18}F-FPT	Amino Acid (tyrosine)	110 minutes	Low tracer uptake in inflammation
^{18}F-FMISO	Hypoxia (nitroimidazole)	110 minutes	Limited data evaluating correlation between avidity and tissue pO_2
^{18}F-EF5	Hypoxia (nitroimidazole)	110 minutes	Detection of tumor hypoxia
^{18}F-FAZA	Hypoxia (nitroimidazole)	110 minutes	Detection of tumor hypoxia, estimation of radiotherapy response

rate constant declined to 0%, and this corresponded with a 58% decrease in the ^{18}F-FDG metabolic rate [15]. This patient experienced complete resolution of the primary tumor completely following chemotherapy. The second sarcoma patient experienced only a 3% reduction in thymidine incorporation, and the metabolic rate of ^{18}F-FDG increased 85% after treatment; this patient rapidly died of progressive disease [15]. This proof of concept study indicated that ^{11}C-thymidine may be a target for future research into sarcoma response to therapy imaging.

^{18}F-Fluoro-3'-deoxy-L-thymidine

^{18}F-Fluoro-3'-deoxy-L-thymidine (^{18}F-FLT) is another radiolabeled thymidine nucleoside analogue which can be used in place of ^{11}C-thymidine. ^{18}F-FLT is taken up by sarcoma cells and incorporated into the thymidine salvage pathway [20]. Once ^{18}F-FLT passively diffuses into the cell [21], it is phosphorylated by the thymidine kinase 1 enzyme (TK1) and trapped in the cell [20]. TK1 activity increases 10-fold when cells undergo DNA synthesis [22], resulting in differential ^{18}F-FLT uptake between proliferating and non-proliferating cells. ^{18}F-FLT-monophosphate can further be phosphorylated to ^{18}F-FLT-triphosphate, but it is not incorporated into DNA due to the substitution of the 5' OH in thymidine by fluorine [17, 20]. Consequently, ^{18}F-FLT PET/CT uptake is an indirect measure of tumor proliferation in cells which undergo DNA replication using the thymidine salvage pathway, although it is a poor measure of proliferation in cells undergoing de novo thymidine synthesis [20]. ^{18}F-FLT PET/CT has advantages over ^{11}C-thymidine. ^{11}C-thymidine requires an onsite cyclotron, limiting its widespread use; however this is not necessary for ^{18}F-FLT [22]. This is because ^{18}F has a half-life of 110 minutes [22], whereas the radiolabeled carbon in ^{11}C-thymidine has a much shorter half-life of 20 minutes and is rapidly metabolized *in vivo* [22, 23]. Consequently, ^{11}C-thymidine PET/CT produces lower quality images which impairs proliferation rate calculations when compared with ^{18}F-FLT PET/CT [22].

Cobben et al. assessed the use of ^{18}F-FLT PET/CT for detection and grading of STS [24]. In a trial of 19 patients with 20 histologically-confirmed STS tumors, all 20 malignant lesions were detected with full body ^{18}F-FLT PET/CT prior to treatment [24]. However the sensitivity of ^{18}F-FDG PET/CT for detecting these sarcomas ranged from 88-92% [24]. Buck et al. imaged 22 patients with established or suspected soft tissue or bone tumors using both ^{18}F-FLT and ^{18}F-FDG PET for pretreatment planning [25]. Seventeen tumors were histologically confirmed to be malignant bone or soft tissue sarcomas, and five tumors were confirmed to be benign. Using a threshold cutoff value of 2.0 for mean SUV, all 17 malignant tumors were identified by ^{18}F-FLT PET (100% sensitivity) and three out of four benign tumors were classified correctly (75% specificity) [25]. However, using this same threshold, one benign lesion was incorrectly classified as malignant by ^{18}F-FLT PET.

^{18}F-FLT PET also compares favorably with ^{18}F-FDG PET as a noninvasive tool to predict sarcoma cell proliferation. In a study of eight RIF-1 sarcoma bearing mice treated with saline or with a single 5 mg/kg dose of cisplatin, normalized uptake of ^{18}F-FLT uptake was linearly correlated with proliferating cell nuclear antigen labeling index ($r=0.89$, $P=0.001$), indicating that ^{18}F-FLT PET avidity is a measure of cell pro-

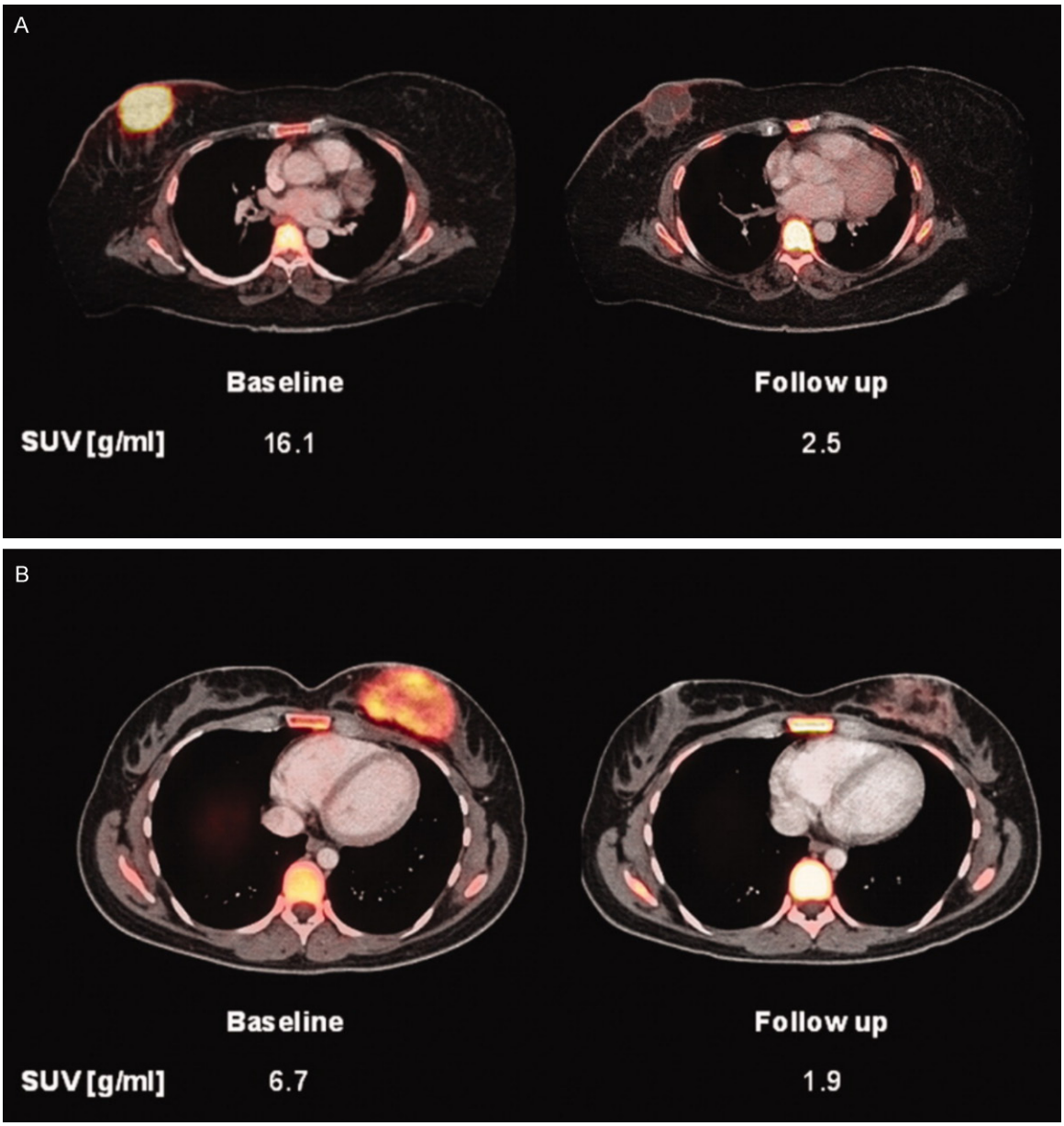

Figure 2. "Baseline and follow-up ^{18}F-FLT positron emission tomography/computed tomography images are shown of 2 patients with angiosarcoma of the breast. The patient shown in (A) exhibited >95% tissue necrosis after neoadjuvant treatment and was classified as a histopathologic responder. The patient in (B) was a histopathologic nonresponder with <5% tissue necrosis after treatment. However, comparable decreases in ^{18}F-FLT uptake of 85% and 71%, respectively, were seen. Therefore, the patient in (B) was misclassified as a metabolic responder by fluorothymidine positron emission tomography analysis. SUV_{peak} indicates peak standardized uptake value". Reprinted, with permission, from reference [27].

liferation *in vivo* [26]. Studies in human patients with sarcoma have also indicated that ^{18}F-FLT PET uptake correlates with histopathologic grade. Buck et al. identified a significant correlation between mean ^{18}F-FLT SUV and histopathologic grade (r=0.71, P=0.01) in 22 human patients with bone and soft tissue sarcoma [25]. Mean ^{18}F-FLT SUV was significantly elevated in high grade sarcomas when compared to low grade sarcomas (mean=6.1, range=2.5-8.3 vs. mean=1.6, range=1.4-1.8; P=0.001) [25]. However, Buck et al. found no correlation between mean ^{18}F-FDG SUV_{max} or SUV_{mean} and sarcoma histologic grade [25]. Another prospective study of 10 patients with locally advanced, nonresectable STS identified a sig-

nificant correlation between sarcoma mitotic index and ^{18}F-FLT SUV_{max} (r=0.87, P=0.001) [17]. Similarly, among 20 histology-confirmed STS in 19 patients, there were significant positive correlations between^{18}F-FLT SUV_{max} and mitotic score (r=0.721, P<0.05), ^{18}F-FLT SUV_{max} and histologic grade (r=0.724, P<0.05), and correlation between tumor-to-nontumor ratio and histologic grade (r=0.747, P<0.05) [24].

^{18}F-FLT PET has also been used to assess sarcoma response to treatment. Benz et al. imaged 20 adult human patients with biopsy-proven, high grade, resectable STS using ^{18}F-FLT PET/CT before and after neoadjuvant therapy [27]. ^{18}F-FLT SUV_{max} decreased from a pretreatment mean of 7.1±3.7 g/mL to 2.7±1.6 g/mL after treatment (P<0.001), indicating a treatment response, and changes in peak FLT uptake were correlated with changes in tumor size (r=0.52, P=0.02) and tumor necrosis (r=0.68, P=0.001) [27]. However, there was no correlation between ^{18}F-FLT uptake and TK1 expression (r=0.26, P=0.27) or Ki-67 activity (r=0.29, P=0.21) [27]. **Figure 2** shows pretreatment and posttreatment ^{18}F-FLT PET images from a histologic responder and a histologic non-responder. ^{18}F-FLT PET can also be used as an early marker of sarcoma response to chemotherapy [26]. Treatment of 8 mice with radiation-induced fibrosarcoma with cisplatin resulted in significant decreases in tumor cell proliferation as measured by a decrease in proliferating cell nuclear antigen labeling index from 14.0%±2.0% to 6.2%±1.0% (P=0.001); this reduction in proliferation was detected by a simultaneous decrease in normalized ^{18}F-FLT uptake in these animals from 0.76±0.08 to 0.51±0.08 (P=0.03) [26]. ^{18}F-FLT PET has also been demonstrated to predict response to therapy in human patients with sarcoma. Van Ginkel et al. report that ^{18}F-FLT SUV_{max} decreased from a mean of 3.5 to 1.7 (P=0.008) and that SUV_{mean} decreased from 1.9 to 0.8 (P=0.002) among 10 patients treated with locally advanced STS treated with hyperthermic isolated limb perfusion, TNF-α, and melphalan [17]. Furthermore, there was a correlation between pretreatment ^{18}F-FLT SUV_{mean} and necrosis following treatment (r=0.642, P<0.05) [17].

^{18}F-FLT PET also potentially has a role in predicting response to targeted therapies. The driving mutation in 85% of Ewing sarcomas is the EWS-FLI1 translocation, which promotes the expression of multiple genes including ENT1, ENT2, and TK1 [28]. ENT1 and ENT2 permit passive transport of ^{18}F-FLT into tumor cells, and TK1 phosphorylates and traps the radiotracer in the cell [28]. Osgood et al. found that repression of EWS-FLI1 in Ewing sarcoma cell lines with small molecule inhibitors reduced mRNA expression of ENT1, ENT2, and TK1 *in vitro*; in contrast, chemotherapeutic agents like 5FU had no effect on TK1 expression [28]. Mice with Ewing sarcoma xenografts were treated with the small molecule inhibitors mithramycin (1 mg/kg), EC-8042 (24 mg/kg), or EC-8105 (1.5 mg/kg), and were subsequently imaged with ^{18}F-FLT PET both before and after therapy [28]. All three agents resulted in significant suppression of ^{18}F-FLT activity (P<0.05), but no suppression was evident after treatment with 5-FU. This suggests that ^{18}F-FLT PET could potentially demonstrate susceptibility and response to targeted EWS-FLI1 therapy for Ewing sarcoma.

Amino acid analogues

^{11}C-methionine

^{11}C-methionine is a radiolabeled amino acid with a half-life of 20.4 minutes [16, 17] and has been investigated as a PET tracer for sarcoma. Its half-life limits its current clinical use. Sarcoma tumor cells upregulate amino acid transport, transmethylation rate, and protein synthesis [29, 30]. Radiolabeled amino acids such as ^{11}C-methionine are absorbed and incorporated into proteins and can serve as a marker of protein synthesis using PET imaging [30]. ^{11}C-methionine was superior to ^{18}F-FDG for differentiating fibrosarcoma from inflammatory background in a mouse model [30]. S180 fibrosarcoma-bearing mice (n=4) were administered full-body PET/CT imaging with either N-(2-[^{18}F]Fluoropropionyl)-L-methionine (FP-MET), FDG, or ^{11}C-methionine [30]. The tumor-to-inflammation ratio of ^{11}C-methionine was 1.64; this was superior to the tumor-to-inflammation ratio of ^{18}F-FDG at 1.14, although the sample size were too small for a robust statistical analysis [30].

^{11}C-methionine may be able to predict outcomes in patients after carbon ion radiotherapy (CIRT) [29]. Sixty-two patients with histologically-confirmed bone or soft tissue sarcomas which were inoperable or who had declined sur-

gery, were imaged using ^{11}C-methionine PET/CT before and up to one month following treatment with carbon ion radiotherapy (CIRT) [29]. Post treatment, ^{11}C-methionine tumor-to-nontumor (T/N) ratio decreased from a mean of 4.58±2.57 to 3.11±2.04 (P=0.00029) [29]. Pretreatment ^{11}C-methionine uptake was predictive of outcome-patients with a pretreatment (T/N) ratio <6 demonstrated significantly higher 2-year survival when compared with patients with higher T/N ratios (69.4% vs. 32.3%, P=0.010). Posttreatment ^{11}C-methionine uptake also had prognostic implications. Patients with a post-treatment T/N ratio of less than 4.4 had better 2-year survival than patients with higher T/N ratios (63.7% vs. 41.3%, P=0.012). A reduction in ^{11}C-methionine T/N ratio of greater than 30% significantly improved 2-year survival (74.6% vs. 41.6%, P=0.049) [29]. The authors concluded that post-CIRT ^{11}C-methionine PET predicted response to therapy and 2-year survival, better than tumor type, size, or stage [29]. However, a separate study found that pretreatment ^{18}F-FDG PET was superior to ^{11}C-methionine for prediction of STS response to neoadjunctive therapy [31]. Nine patients with STS were imaged with ^{18}F-FDG and ^{11}C-methionine PET/CT before and after neoadjuvant chemoradiotherapy [31]. Using a cutoff of 45% SUV_{max}, ^{18}F-FDG PET was able to distinguish between partial and complete responders to therapy (complete responders defined by the authors as 91-100% tumor necrosis on histology post-therapy) [31]. In contrast, it was not possible to differentiate partial and complete responders using change in SUV_{max} with ^{11}C-methionine [31].

N-(2-[^{18}F]-fluoropropionyl)-L-methionine

^{18}F-FPMET is an ^{18}F-labeled radiolabeled amino acid with a half-life of 110 minutes [22] that has been used to measure tumor amino acid uptake. ^{18}F-FPMET differs from ^{11}C-methionine because it not incorporated into protein in S180 mouse fibrosarcoma models [30]. Methionine uptake is upregulated in sarcomas, therefore ^{18}F-FPMET should preferentially be taken into tumor cells via sodium-dependent transporters as a result [29, 30]. Preliminary evidence indicates that ^{18}F-FPMET PET has a comparable ability to distinguish tumor from inflammatory background as ^{11}C-methionine PET [30]. Among mice with fibrosarcoma imaged with PET/CT using either ^{18}F-FPMET or ^{11}C-methionine, ^{18}F-FPMET demonstrated a tumor-to-inflammation ratio of 1.64 compared to 1.62 for ^{11}C-methionine [30]. However, ^{18}F-FPMET has yet to be studied in the clinical setting, possibly because it is a measure of amino acid uptake rather than protein incorporation.

Cis-4-[^{18}F]-fluoro-L-proline

Cis-4-[^{18}F]-Fluoro-L-proline (^{18}F-FPro) is an amino acid analog. Sarcomas are mesenchymal tumors, so they have been hypothesized to highly express collagen. Proline is a major component of collagen; therefore sarcomas would be expected to demonstrate high levels of ^{18}F-FPro uptake and protein incorporation [32]. *In vivo* mouse models of osteosarcoma indicate that cis-^{18}F-FPro accumulates within osteosarcoma tumor cells [33]. Transplanted osteosarcoma tumors in mice demonstrated a maximum tumor cis-^{18}F-FPro uptake of 11.9% injected dose per gram (ID/g) (n=7, sd=2.19) four hours after cis-^{18}F-FPro infusion, whereas blood pool demonstrated an uptake of 2.86% ID/g (n=7, sd=0.29) [33]. High cis-^{18}F-FPro uptake was also present in liver the (9.77% ID/g, sd=0.85), kidney (46.9% ID/g, sd=3.2), and pancreas (19.0% ID/g, sd=1.83) at the same time point [33]. Cis-^{18}F-FPro uptake within sarcomas largely reflected amino acid transport rather than protein incorporation as only 33±7% of cis-^{18}F-FPro activity was protein-bound after one hour [33]. Stoeffuls et al. imaged eight human patients with peripheral tumors, including one patient with Ewing sarcoma, using cis-^{18}F-FPro and ^{18}F-FDG PET. Cis-^{18}F-FPro uptake in each tumor was significantly lower than the ^{18}F-FDG SUV (1.7±0.6 vs. 5.7±3.0, P=0.01), and the Ewing sarcoma lesion exhibited a similar level of uptake as the liver and therefore was only faintly visible using cis-^{18}F-FPro [32].

L-[1-^{11}C]-tyrosine

^{11}C-tyrosine is a radiolabeled amino acid that is incorporated into protein by tumor cells and has a half-life of 20 minutes [34]. ^{11}C-tyrosine has been investigated as a PET tracer to measure protein synthesis rate (PSR) in STS [5]. ^{11}C-tyrosine PET detects protein synthesis rather than glucose metabolism. ^{11}C-tyrosine PET in theory should distinguish local inflammation from viable sarcoma, because protein synthe-

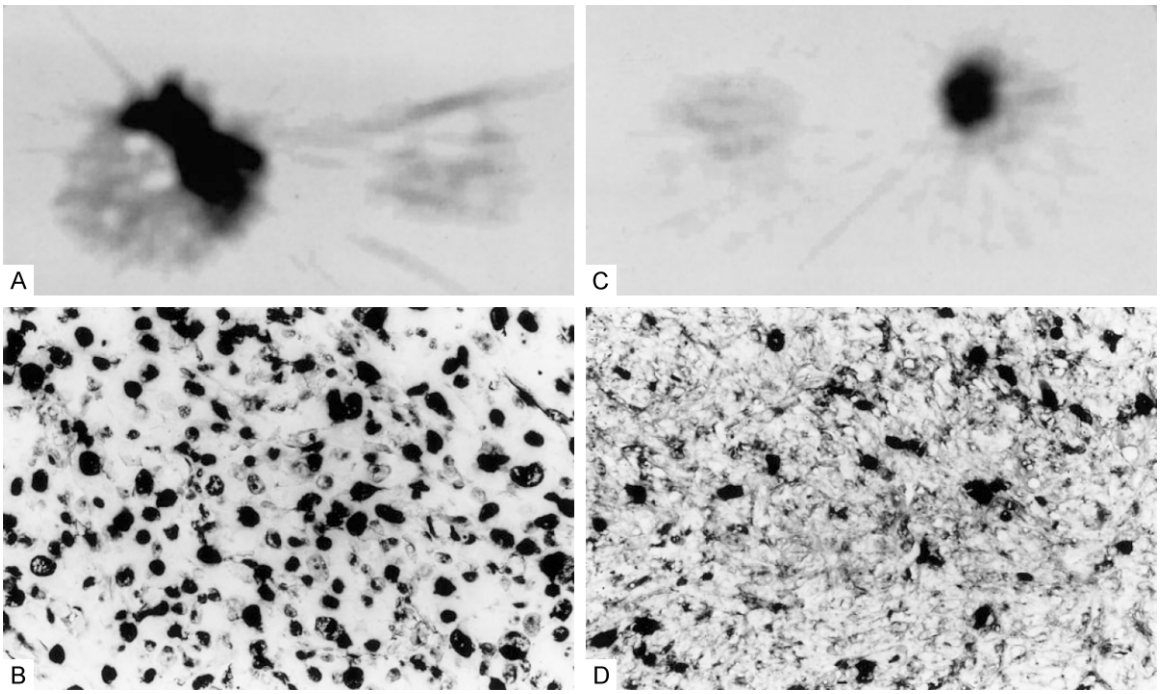

Figure 3. (A) "^{11}C-tyrosine PET image of a sarcoma not otherwise specified with a relatively high PSR and (B) corresponding MIB-1 stained tissue section (400×) of the tumor showing a high number of proliferating cells. All dark nuclei express Ki-67 and have entered the cell cycle. (C) ^{11}C-tyrosine PET image of a malignant schwannoma with a relatively low PSR and (D) corresponding MIB-1 stained tissue section (400×) showing a low number of proliferating cells". Reprinted, with permission, from reference [5].

sis is relatively low in many inflammatory cells such as neutrophils when compared with sarcomas [5, 33, 35]. ^{11}C-tyrosine should be able to identify proliferative tumors in highly metabolically-active tissues (such as brain) that use glucose by detecting protein synthesis [34]. Protein production increases throughout the cell cycle, so elevated PSR in tumors may be indicative of tumor proliferation [5]. ^{11}C-tyrosine uptake is related to histopathologic measures of proliferation [5]. Twenty-one patients with untreated, histologically-diagnosed STS were imaged using ^{11}C-tyrosine to estimate PSR [5]. Sarcoma tissue was harvested by incisional biopsy of viable tumor within 8 weeks to assess histological grade, differentiation, mitotic index, and Ki-67 expression (see **Figure 3**) [5]. No correlation was found between sarcoma grade and the maximum protein synthesis rate (PSR_{max}) or average protein synthesis rate (PSR_{ave}) values derived from ^{11}C-tyrosine imaging, possibly because increased tumor necrosis, which increases histologic grade, lowers the PSR [5]. However, there was a significant correlation between PSR_{ave} and mitoses (R=0.67, P<0.001), PSR_{ave} and Ki-67 proliferative index (R=0.54, P<0.05), PSR_{max} and mitoses (R=0.64, P<0.01), and PSR_{max} and Ki-67 proliferative index (R=0.54, P<0.05) [5].

^{11}C-tyrosine has also been assessed as a marker of tumor response to treatment. Van Ginkel et al. treated 12 patients with locally advanced, biopsy-proven STS with neoadjuvant rTNF-a and melphalan therapy using hyperthermic isolated limb perfusion techniques [35]. Patients were imaged with ^{11}C-tyrosine PET prior to limb perfusion, two weeks after completion of neoadjuvant treatment, and at 8 weeks post therapy and PSR was calculated [35]. There was no significant difference in pretreatment PSR in partial pathologic response patients (defined as viable tumor at resection) and complete response patients (defined as no viable tumor at resection) [35]. However, patients with complete responses demonstrated significant decreases in PSR pretreatment at week 2 (P<0.05) and at week 8 (P<0.05) posttreatment, suggesting that PSR estimated from ^{11}C-tyrosine PET can assess response to therapy [35].

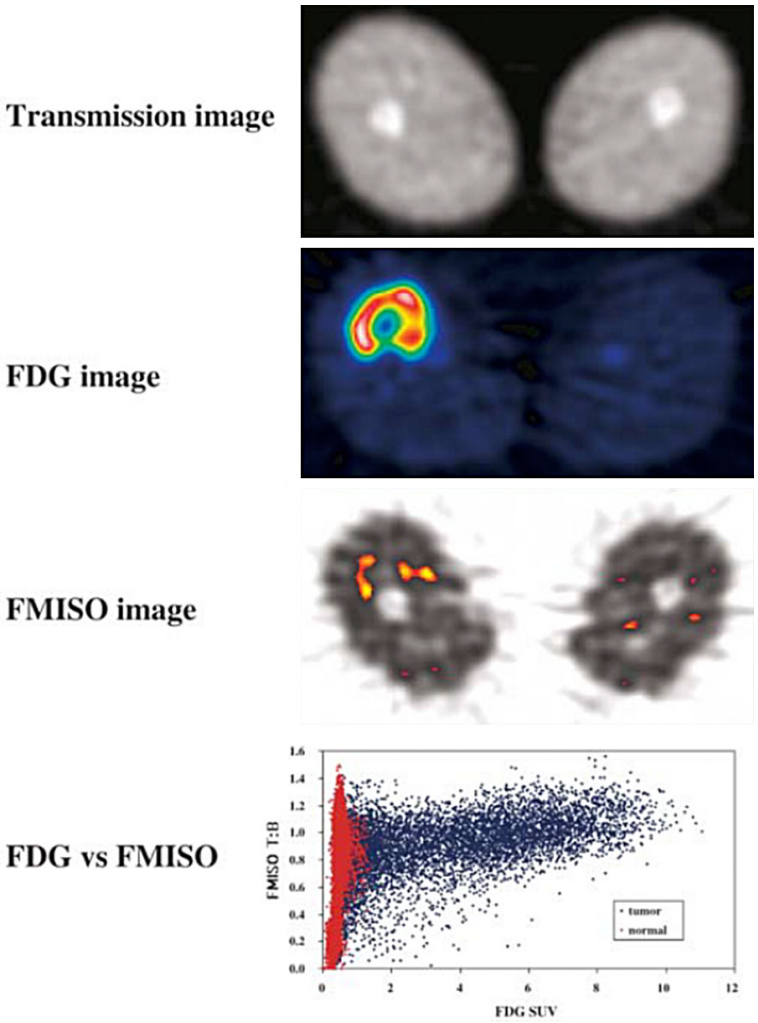

Figure 4. "^{18}F-FDG and ^{18}F-FMISO scans (with an attenuation scan for localization) of a grade 2 osteosarcoma of the right femur. The ^{18}F-FMISO image shows pixels with a tissue to blood ratio ≥1.2 in color. The correlation of ^{18}F-FDG vs ^{18}F-FMISO using pixel-by-pixel analysis was r=0.48 for the whole tumor". Reprinted, with permission, from reference [47].

O-(3-[^{18}F]-fluoropropyl)-L-tyrosine

O-(3-[^{18}F]-fluoropropyl-L-tyrosine (^{18}F-FPT) is another ^{18}F-labelled amino acid radiotracer which has been investigated for PET imaging of sarcoma. Tang et al. demonstrated that ^{18}F-FPT PET is able to detect tumor and to differentiate tumor from inflammation in a mouse model of fibrosarcoma [36]. Fifteen mice were inoculated with S18 fibrosarcoma, and fifteen mice were inoculated with *Staphylococcus aureus* as a model of inflammation [36]. Animals were imaged using ^{18}F-FPT PET and ^{18}F-FDG PET 7-14 days after fibrosarcoma inoculation or 72 hours after S. *aureus* inoculation [36]. ^{18}F-FPT uptake is not increased by inflammation; there was no significant difference in ^{18}F-FPT uptake between the inflammatory abscess and the contralateral muscle in S. *aureus*-infected mice [36]. By contrast, the ratio of ^{18}F-FDG uptake between inflammatory abscesses and contralateral muscle was 4.0:1 (P<0.05) [36]. Fibrosarcoma tumors also demonstrated significant ^{18}F-FPT uptake; the differential uptake ratio (DUR) of fibrosarcoma tissue at 90 minutes was 0.98±0.19, whereas the mean DUR of contralateral muscle in these animals was 0.34±0.10 (P<0.05) [36].

Hypoxia pet radiotracers

Tumor hypoxia is an important factor in sarcoma prognosis because it is associated with poor response to radiotherapy [37, 38], higher local recurrence rate, higher rate of developing pulmonary metastases and death [37, 39]. Hypoxia within sarcomas leads to activation of hypoxia-inducible factors that upregulate the pathways responsible for tumor angiogenesis and metastasis [40]. Eppendorf electrodes placed directly into tissues to measure the partial pressure of oxygen (pO_2) are the gold standard for measuring tissue hypoxia; however, this technique is invasive and can only measure one region within a tumor [41]. Hypoxia imaging allows for non-invasive global measurement of sarcoma hypoxia [41].

^{18}F-fluoromisonidazole (^{18}F-FMISO) is a radiolabeled nitroimidazole, which preferentially accumulates in hypoxic cells [37]. In preclinical trials, ^{18}F-FMISO PET demonstrated superior tumor-to-inflammation ratios than ^{18}F-FDG PET in a KHT-sarcoma-bearing and inflammation-bearing mouse models [42]. Intratumor hypoxic volumes determined by ^{18}F-FMISO PET are

highly correlated with hypoxic volume demonstrated by pimonidazole-immunohistochemistry in rat models of rhabdomyosarcoma [43]. ^{18}F-FMISO PET has also been used to identify tumor hypoxia in spontaneous canine bone and soft tissue sarcomas (confirmed by Eppendorf needle electrode measurement of pO_2) [44]. ^{18}F-FMISO PET imaging in human patients with sarcoma has been less promising. A trial of 18 patients, including nine with STS, found no correlation between ^{18}F-FMISO PET tumor-to-muscle ratios and Eppendorf pO_2 measurements [45]. A separate study involving six patients with histologically-confirmed STS also found no correlation between ^{18}F-FMISO PET tumor-to-muscle ratio and Eppendorf measurements [46]. Although three tumors demonstrated extensive hypoxia in that study, only one demonstrated accumulation of ^{18}F-FMISO [46]. A third study of 19 patients with STS found no correlations between pretreatment ^{18}F-FMISO PET-derived hypoxic volume and tumor size, grade, ^{18}F-FDG PET SUV_{max}, or VEGF expression (see **Figure 4**) [47].

2-(2-nitro-1H-imidazol-1-yl)-N-(2,2,3,3,3-^{18}F-pentafluoropropyl)-acetamide (^{18}F-EF5) is a radiolabeled hypoxia tracer with contains a 2-nitroimidazole moiety, permitting selective uptake in hypoxic cells [48]. Unlabeled EF5 has been well established as an immunohistochemical marker of hypoxia [48, 49], and it has been associated with the presence of mitoses and higher histologic grade in human patients with STS [49]. ^{18}F-EF5 has been tested in humans and was determined to be safe with an acceptable level of radiation exposure [50], and ^{18}F-EF5 PET has been validated for the assessment of hypoxia in head and neck cancers [51]. This tracer has not yet been studied in human sarcomas, but ^{18}F-EF5 PET detected hypoxia in one of two cats with histologically-confirmed fibrosarcomas [52].

^{18}F-1-(5-fluoro-5-deoxy-α-D-arabinofuranosyl)-2-nitroimidazole (^{18}F-FAZA) is another radiolabeled nitroimidazole derivative which may be used in place of ^{18}F-FMISO. An advantage of ^{18}F-FAZA over ^{18}F-FMISO is faster washout from tissues [53, 54]; however, the tradeoff is lower tracer uptake by tumors and a lower sensitivity of ^{18}F-FAZA PET for the detection of hypoxic regions in rat carcinosarcoma models [54]. ^{18}F-FAZA PET accurately reflected tumor hypoxia in rat models of rhabdomyosarcoma. ^{18}F-FAZA PET tumor-to-blood ratios were strongly correlated with pO_2 as determined by Eppendorf oximetry (r=0.93) [55], and ^{18}F-FAZA luminescent activity was also correlated with pimonidazole (a histological marker of hypoxia) fluorescence [53]. ^{18}F-FAZA may be able to guide therapy decisions in the future. Mice with hypoxic sarcomas with higher tumor-to-blood ratios benefited from combined treatment of radiotherapy and nimorazole (a hypoxic radiosensitizer that generates free radicals to produce radiation damage), whereas this benefit was not seen in mice with less hypoxic sarcomas [56, 57]. ^{18}F-FAZA PET can also guide decisions about the use of carbogen breathing and dose escalation in radiotherapy in mouse models of rhabdomyosarcoma [41].

Discussion

Nucleoside analogs, amino acid analogs, and hypoxia PET tracers are currently undergoing evaluation in preclinical studies as potential complements to traditional ^{18}F-FDG sarcoma imaging.

^{18}F-labelled compounds are probably the most likely to be used in clinical practice in future because of the relatively long half-life of ^{18}F. ^{18}F-FLT is likely the best radiotracer to evaluate DNA synthesis in sarcoma. ^{18}F-FPT is probably the best radiotracer to study protein synthesis in sarcoma given the preclinical performance and relatively long half-life. All three hypoxia tracers have various merits. ^{18}F-EF5 has the additional benefit of being able to be directly correlated with uptake from cold EF5. However, ^{18}F-EF5 synthesis is more complicated than that for ^{18}F-FMISO. An advantage of ^{18}F-FAZA over ^{18}F-FMISO is faster washout from tissues however, this results in lower tracer uptake by tumors and a lower sensitivity of ^{18}F-FAZA PET for the detection of hypoxic regions.

What we have learned is that there is significant heterogeneity within and between sarcomas. DNA synthesis, measured using ^{11}C-thymidine or ^{18}F-FLT, showed significant differences between sarcomas; and the change in DNA synthesis after treatment could predict change in tumor size, necrosis and patient clinical course. DNA synthesis was also correlated with sarcoma grade and mitotic index. However, DNA synthesis was not correlated with cellular proliferation measured by Ki-67 activity.

In contrast, protein synthesis was not correlated with sarcoma grade. Protein synthesis was correlated with increased mitotic figures, and cellular proliferation measured by Ki-67 activity. Change in protein synthesis was also correlated with response to therapy and predicted overall survival better than tumor size, grade or tumor stage. The previously published reports suggest that not all DNA synthesis results in protein synthesis; however, both DNA and protein synthesis were predictors of outcome in patients with sarcoma. It is unclear how strongly protein synthesis is correlated with collagen synthesis. Collagen synthesis measured by cis-^{18}F-FPro uptake varied between sarcoma subtype with significant uptake in osteosarcoma and uptake similar to background in Ewing's sarcoma.

Like protein synthesis, hypoxia was not correlated with tumor grade, and was not correlated with tumor size, glycolysis or VEGF. This suggests that hypoxia imaging provides information about the tumor biology beyond that captured by ^{18}F-FDG PET/CT. This also suggests that DNA synthesis seems independent of sarcoma hypoxia. Hypoxia imaging has been limited, however, by poor correlation between ^{18}F-FMISO avidity and Eppendorf pO_2 measurements. ^{18}F-FAZA and ^{18}F-EF5 are promising new hypoxia radiotracers, and preclinical evidence has demonstrated correlation between EF5 and FAZA deposition with histologic and Eppendorf measurements of hypoxia respectively. The presence and extent of hypoxia imaging may allow clinicians to predict response to radiotherapy and thereby guide clinical decision making.

Radiolabeled nanoparticles may provide a new direction for investigation in sarcoma imaging. Nanoparticles are self-assembling inorganic compounds which can accumulate in tumors by passing through aberrant, more permeable blood vessels within tumors or by directly binding tumor targets [58]. Radiolabeled nanoparticle PET has not been assessed in sarcoma; however, this technology has been investigated for tumor detection and for assessment of angiogenesis [59] and may provide clinically useful information about tumor perfusion.

The ability to quantitatively assess tumor DNA synthesis, tumor protein synthesis, and tumor hypoxia *in vivo* will help clinicians better understand underlying sarcoma biology. Several of these tracers have shown already shown promise in the preclinical setting to predict sarcoma prognosis and response to therapy. These targeted PET tracers have the potential to be increasingly used in the era of precision and personalized medicine. The use and development of targeted therapies for sarcoma has been limited due to the rarity and heterogeneity of these tumors. These tumors are very heterogeneous and sometimes subject to sampling error from biopsies. Imaging tracers have the potential to transform clinical management, because imaging can provide global characterization of sarcomas and are not subject to sampling error. The additional information from these novel tracers will better inform patient treatment and in the future ultimately improve patient outcomes.

Disclosure of conflict of interest

None.

Address correspondence to: Dr. Ronnie Sebro, Department of Radiology, University of Pennsylvania, 3400 Spruce Street, Philadelphia, PA 19104, USA. Tel: 215-294-9512; E-mail: Ronnie.sebro@uphs.upenn.edu

References

[1] Chen PH, Mankoff DA, Sebro RA. Clinical overview of the current state and future applications of positron emission tomography in bone and soft tissue sarcoma. Clin Transl Imaging 2017; 5: 343-3588.

[2] Fisher SM, Joodi R, Madhuranthakam AJ, Öz OK, Sharma R, Chhabra A. Current utilities of imaging in grading musculoskeletal soft tissue sarcomas. Eur J Radiol 2016; 85: 1336-1344.

[3] Bielack SS, Kempf-Bielack B, Delling G, Exner GU, Flege S, Helmke K, Kotz R, Salzer-Kuntschik M, Werner M, Winklemann W, Zoubek A, Jürgens H, Winkler K. Prognostic factors in high-grade osteosarcoma of the extremities or trunk: an analysis of 1,702 patients treated on neoadjuvant cooperative osteosarcoma study group protocols. J Clin Oncol 2002; 20: 776-790.

[4] Maretty-Nielsen K. Prognostic factors in soft tissue sarcoma. Dan Med J 2014; 61: B4957.

[5] Plaat B, Kole A, Mastik M, Hoekstra H, Molenaar W, Vaalburg W. Protein synthesis rate measured with L-[1-^{11}C]tyrosine positron emission tomography correlates with mitotic activity and MIB-1 antibody-detected proliferation in

human soft tissue sarcomas. Eur J Nucl Med 1999; 26: 328-332.
[6] Casali PG, Blay JY, Bertuzzi A, Bielack S, Bjerkehagen B, Bonvalot S, Boukovinas I, Bruzzi P, Dei Tos AP, Dileo P, Eriksson M, Fedenko A, Ferrari A, Ferrari S, Gelderblom H, Grimer R, Gronchi A, Haas R, Hall KS, Hohenberger P, Issels R, Joensuu H, Judson I, Le Cesne A, Litière S, Martin-Broto J, Merimsky O, Montemurro M, Morosi C, Picci P, Ray-Coquard I, Reichardt P, Rutkowski P, Schlemmer M, Stacchiotti S, Torri V, Trama A, Van Coevorden F, Van der Graaf W, Vanel D, Wardelmann E, Bolle S, Capanna R, Delaney T, Doglietto F, Fossati P, Jeys L, Kasper B, Leithner A, Radaelli S, Scheipl S, Tamborini E, Uhl M, Vleggert-Lankamp CL. Bone sarcomas: ESMO clinical practice guidelines for diagnosis, treatment and follow-up. Ann Oncol 2014; 25: iii113-iii123.
[7] Eary JF, O'Sullivan F, O'Sullivan J, Conrad EU. Spatial heterogeneity in sarcoma ^{18}F-FDG uptake as a predictor of patient outcome. J Nucl Med 2008; 49: 1973-1979.
[8] Eary JF, Mankoff DA. Tumor metabolic rates in sarcoma using FDG PET. J Nucl Med 1998; 39: 250-254.
[9] Eary JF, Conrad EU, Bruckner JD, Folpe A, Hunt KJ, Mankoff DA, Howlett AT. Quantitative [F-18] fluorodeoxyglucose positron emission tomography in pretreatment and grading of sarcoma. Clin Cancer Res 1998; 4: 1215-1220.
[10] Eary JF, O'Sullivan F, Powitan Y, Chandhury KR, Vernon C, Bruckner JD, Conrad EU. Sarcoma tumor FDG uptake measured by PET and patient outcome: a retrospective analysis. Eur J Nucl Med Mol Imaging 2002; 29: 1149-1154.
[11] O'Sullivan F, Roy S, Eary J. A statistical measure of tissue heterogeneity with application to 3D PET sarcoma data. Biostatistics 2003; 4: 433-448.
[12] O'Sullivan F, Roy S, O'Sullivan J, Vernon C, Eary J. Incorporation of tumor shape into an assessment of spatial heterogeneity for human sarcomas imaged with FDG-PET. Biostatistics 2005; 6: 293-301.
[13] Choi YY, Kim JY, Yang SO. PET/CT in benign and malignant musculoskeletal tumors and tumor-like conditions. Semin Musculoskelet Radiol 2014; 18: 133-148.
[14] Subhawong TK, Winn A, Shemesh SS, Pretell-Mazzini J. F-18 FDG PET differentiation of benign from malignant chondroid neoplasms: a systematic review of the literature. Skeletal Radiol 2017; 46: 1233-1239.
[15] Shields AF, Mankoff DA, Link JM, Graham MM, Eary JF, Kozawa SM, Zheng M, Lewellen B, Lewellen TK, Grierson JR, Krohn KA. Carbon-11-thymidine and FDG to measure therapy response away regional metabolism. J Nucl Med 1998; 39: 1757-1762.
[16] Bading JR, Shields AF. Imaging of cell proliferation: status and prospects. J Nucl Med 2008; 49: 64S-80S.
[17] Been LB, Suurmeijer AJ, Elsinga PH, Jager PL, van Ginkel RJ, Hoekstra HJ. ^{18}F-fluorodeoxythymidine PET for evaluating the response to hyperthermic isolated limb perfusion for locally advanced soft-tissue sarcomas. J Nucl Med 2007; 48: 367-372.
[18] Shields AF, Graham MM, Kozawa SM, Kozell LB, Link JM, Swenson ER, Spence AM, Bassingthwaighte JB, Krohn KA. Contribution of labeled carbon dioxide to PET imaging of carbon-11-labeled compounds. J Nucl Med 1992; 33: 581-584.
[19] Eary JF, Link JM, Muzi M, Conrad EU, Mankoff DA, White JK, Krohn KA. Multiagent PET for risk characterization in sarcoma. J Nucl Med 2011; 52: 541-546.
[20] Mckinley ET, Ayers GD, Smith RA, Saleh SA, Zhao P, Washington MK, Coffey RJ, Manning HC. Limits of [^{18}F]-FLT PET as a biomarker of proliferation in oncology. PLoS One 2013; 8: 1-9.
[21] Plotnick DA, Emerick LE, Krohn KA, Unadkat JD, Schwartz JL. Different modes of transport for 3H-thymidine, 3H-FLT, and 3H-FMAU in proliferating and nonproliferating human tumor cells. Nano 2008; 6: 2166-2171.
[22] Shields AF, Grierson JR, Dohmen BM, Machulla HJ, Stayanoff JC, Lawhorn-Crews JM, Obradovich JE, Muzik O, Mangner TJ. Imaging proliferation in vivo with [F-18]FLT and positron emission tomography. Nat Med 1998; 4: 1334-1336.
[23] Perumal M, Pillai RG, Barthel H, Leyton J, Latigo JR, Forster M, Mitchell F, Jackman AL, Aboagye EO. Redistribution of nucleoside transporters to the cell membrane provides a novel approach for imaging thymidylate synthase inhibition by positron emission tomography. Cancer Res 2006; 66: 8558-8564.
[24] Cobben DC, Elsinga PH, Suurmeijer AJ, Vallburg W, Maas B, Jager PL, Hoekstra HJ. Detection and grading of soft tissue sarcomas of the extremities with ^{18}F-3'-fluoro-3'-deoxy-L-thymidine. Clin Cancer Res 2004; 10: 1685-1690.
[25] Buck AK, Herrmann K, Büschenfelde CM, Juweid ME, Bischoff M, Glatting G, Weirich G, Möller P, Wester HJ, Scheidhauer K, Dechow T, Peschel C, Schwaiger M, Reske SN. Imaging bone and soft tissue tumors with the proliferation marker [^{18}F] fluorodeoxythymidine. Clin Cancer Res 2008; 14: 2970-2977.
[26] Leyton J, Latigo JR, Perumal M, Dhaliwal H, He Q, Aboagye EO. Early detection of tumor re-

sponse to chemotherapy by 3'-deoxy-3'-[^{18}F] fluorothymidine positron emission tomography: the effect of cisplatin on a fibrosarcoma tumor model in vivo. Cancer Res 2005; 65: 4202-4210.

[27] Benz MR, Czernin J, Allen-Auerbach MS, Dry SM, Sutthiruangwong P, Spick C, Radu C, Weber WA, Tap WD, Eiber FC. 3'-Deoxy-3'-[^{18}F] Fluorothymidine positron emission tomography for response assessment in soft tissue sarcoma: a pilot study to correlate imaging findings with tissue thymidine kinase 1 and Ki-67 activity and histopathologic response. Cancer 2012; 118: 3135-3144.

[28] Osgood CL, Tantawy MN, Maloney N, Madaj ZB, Peck A, Boguslawski E, Jess J, Buck J, Winn ME, Manning HC, Grohar PJ. ^{18}F-FLT positron emission tomography (PET) is a pharmacodynamic marker for EWS-FLI1 activity and Ewing sarcoma. Sci Rep 2016; 6: 1-10.

[29] Zhang H, Yoshikawa K, Tamura K, Tomemori T, Sagou K, Tian M, Kandatsu S, Kamada T, Tsuji H, Suhara T, Suzuki K, Tanada S, Tsugii H. [^{11}C] methionine positron emission tomography and survival in patients with bone and soft tissue sarcomas treated by carbon ion radiotherapy. Clin Cancer Res 2004; 10: 1764-1772.

[30] Hu KZ, Wang H, Huang T, Tang G, Liang X, He S, Tang X. Synthesis and biological evaluation of N-(2-[^{18}F]Fluoropropionyl)-L-methionine for tumor imaging. Nucl Med Biol 2013; 40: 926-932.

[31] Ghigi G, Micera R, Maffione AM, Castellucci P, Cammelli S, Ammendolia I, Nanni C, Barbieri E, Grassetto G, Fanti S, Rubello D. ^{11}C-Methionine vs. ^{18}F-FDG PET in soft tissue sarcoma patients treated with neoadjuvant therapy: preliminary results. In Vivo 2009; 23: 105-110.

[32] Stoffels G, Pauleit D, Haas R, Kobbe G, Salber D, Hamacher K, Coenen HH, Langen KJ. cis-4-[^{18}F]-Fluoro-l-proline fails to detect peripheral tumors in humans. Nucl Med Biol 2008; 35: 895-900.

[33] Wester HJ, Herz M, Senekowitsch-Schmidtke R, Schwaiger M, Stöcklin G, Hamacher K. Preclinical evaluation of 4-[^{18}F]fluoroprolines: diastereomeric effect on metabolism and uptake in mice. Nucl Med Biol 1999; 26: 259-265.

[34] Paans M, Pruim J, van Waarde A, Willemsen T, Vaalburg W. Radiolabelled-tyrosine for the measurement of protein synthesis rate in vivo by positron emission tomography. Baillieres Clin Endocrinol Metab 1996; 10: 497-510.

[35] van Ginkel RJ, Kole AC, Nieweg OE, Molenaar WM, Pruim J, Koops HS, Vaalburg W, Hoekstra HJ. L-[1-^{11}C]-tyrosine PET to evaluate response to hyperthermic isolated limb perfusion for locally advanced soft-tissue sarcoma and skin cancer. J Nucl Med 1999; 40: 262-267.

[36] Tang G, Wang M, Tang X, Luo L, Gan M. Synthesis and evaluation of O-(3-[^{18}F]fluoropropyl)-L-tyrosine as an oncologic PET tracer. Nucl Med Biol 2003; 30: 733-739.

[37] Rajendran JG, Mankoff DA, Sullivan FO, Peterson LM, Schwartz DL, Conrad EU, Spence AM, Muzi M, Farwell DG, Krohn KA. Hypoxia and glucose metabolism in malignant tumors: evaluation by [^{18}F] fluoromisonidazole and [^{18}F] fluorodeoxyglucose positron emission tomography imaging hypoxia and glucose metabolism in malignant tumors: evaluation by [^{18}F] fluoromisonidazol. Clin Cancer Res 2004; 10: 2245-2252.

[38] Qian Y, Von Eyben R, Liu Y, Chin FT, Miao Z, Apte S, Carter JN, Binkley MS, Pollom EL, Harris JP, Prionas ND, Kissel M, Simmons A, Diehn M, Shultz DB, Brown HM, Maxim PG, Koong AC, Graves EE, Loo BW Jr. ^{18}F-EF5 PET-based imageable hypoxia predicts local recurrence in tumors treated with highly conformal radiation therapy. Int J Radiat Oncol Biol Phys 2018; 102: 1-10.

[39] Brizel DM, Scully SP, Harrelson JM, Layfield LJ, Bean JM, Prosnitz LR, Dewhirst MW. Tum-or oxygenation predicts for the likelihood of distant metastases in human soft tissue sarcoma tumor oxygenation predicts for the likelihood of distant metastases in human soft tissue sarcoma. Cancer Res 1996: 56; 941-943.

[40] Semenza GL. Hypoxia-inducible factors: mediators of cancer progression and targets for cancer therapy. Trends Pharmacol Sci 2013; 33: 207-214.

[41] Tran LB, Bol A, Labar D, Karroum O, Bol V, Jordan B, Gregoire V, Gallez B. Potential role of hypoxia imaging using ^{18}F-FAZA PET to guide hypoxia-driven interventions (carbogen breathing or dose escalation) in radiation therapy. Radiother Oncol 2014; 113: 204-209.

[42] Liu RS, Chou TK, Chang CH, Wu CY, Chang CW, Chang TJ, Wang SJ, Lin WJ, Wang HE. Biodistribution, pharmacokinetics and PET Imaging of [^{18}F]FMISO, [^{18}F]FDG and [^{18}F]FAc in a sarcoma- and inflammation-bearing mouse model. Nucl Med Biol 2009; 36: 305-312.

[43] Dubois L, Landuyt W, Haustermans K, Dupont P, Bormans G, Vermaelen P, Flamen P, Verbeken E, Mortelmans L. Evaluation of hypoxia in an experimental rat tumour model by [^{18}F] fluoromisonidazole PET and immunohistochemistry. Br J Cancer 2004; 91: 1947-1954.

[44] Bruehlmeier M, Kaser-Hotz B, Achermann R, Bley CR, Wergin M, Schubiger PA, Ametamey SM. Measurement of tumor hypoxia in spontaneous canine sarcomas. Vet Radiol Ultrasound 2005; 46: 348-354.

[45] Mortensen LS, Buus S, Nordsmark M, Bentzen L, Munk OL, Keiding S, Overgaard J. Identifying

hypoxia in human tumors: a correlation study between ^{18}F-FMISO PET and the eppendorf oxygen-sensitive electrode. Acta Oncol (Madr) 2010; 49: 934-940.

[46] Bentzen L, Keiding S, Nordsmark M, Falborg L, Hansen SB, Keller J, Nielsen OS, Overgaard J. Tumour oxygenation assessed by ^{18}F-fluoromisonidazole PET and polarographic needle electrodes in human soft tissue tumours. Radiother Oncol 2003; 67: 339-344.

[47] Rajendran JG, Wilson DC, Conrad EU, Peterson LM, Bruckner JD, Rasey JS, Chin LK, Hofstrand PD, Grierson JR, Eary JF, Krohn KA. [^{18}F]FMISO and [^{18}F]FDG PET imaging in soft tissue sarcomas: Correlation of hypoxia, metabolism and VEGF expression. Eur J Nucl Med Mol Imaging 2003; 30: 695-704.

[48] Chitneni SK, Bida GT, Zalutsky MR, Dewhirst MW. Comparison of the hypoxia PET Tracer ^{18}F-EF5 to immunohistochemical marker EF5 in 3 different human tumor xenograft models. J Nucl Med 2017; 4: 1192-1197.

[49] Evans SM, Fraker D, Hahn SM, Gleason K, Jenkins WT, Jenkins K, Hwang WT, Zhang P, Mick R, Koch CJ. EF5 binding and clinical outcome in human soft tissue sarcomas. Int J Radiat Oncol Biol Phys 2006; 64: 922-927.

[50] Lin LL, Silvoniemi A, Stubbs JB, Rengan R, Suilamo S, Solin O, Divgi C, Eskola O, Sorger JM, Stabin MG, Kachur A, Hahn SM, Grönroos TJ, Forsback S, Evans SM, Koch CJ, Minn H. Radiation dosimetry and biodistribution of the hypoxia tracer ^{18}F-EF5 in oncologic patients. Cancer Biother Radiopharm 2012; 27: 412-419.

[51] Silvoniemi A, Suilamo S, Laitinen T, Forsback S. Repeatability of tumour hypoxia imaging using [^{18}F]-EF5 PET/CT in head and neck cancer. Eur J Nucl Med Mol Imaging 2017; 45: 161-169.

[52] Allemann K, Wyss MT, Wergin M, Ohlerth S, Rohrer-Bley C, Evans SM, Schubiger AP, Ametamey SM, Kaser-Hotz B. Measurements of hypoxia ([^{18}F]-FMISO, [^{18}F]-EF5) with positron emission tomography (PET) and perfusion using PET ([150]-H_2O) and power doppler ultrasonography in feline fibrosarcomas*. Vet Comp Oncol 2005; 3: 211-221.

[53] Busk M, Horsman MR, Jakobsen S, Keiding S, van der Kogel AJ, Bussink J, Overgaard J. Imaging hypoxia in xenografted and murine tumors with ^{18}f-fluoroazomycin arabinoside: a comparative study involving microPET, autoradiography, PO2-polarography, and fluorescence microscopy. Int J Radiat Oncol Biol Phys 2008; 70: 1202-1212.

[54] Sorger D, Patt M, Kumar P, Wiebe LI, Barthel H, Seese A, Dannenberg C, Tannapfel A, Kluge R, Sabri O. [^{18}F]Fluoroazomycinarabinofuranoside (^{18}FAZA) and [^{18}F]Fluoromisonidazole (^{18}FMISO): a comparative study of their selective uptake in hypoxic cells and PET imaging in experimental rat tumors. Nucl Med Biol 2003; 30: 317-326.

[55] Tran LB, Bol A, Labar D, Jordan B, Magat J, Mignion L, Gregoire V, Gallez B. Hypoxia imaging with the nitroimidazole ^{18}F-FAZA PET tracer: a comparison with oxyLite, EPR oximetry and 19F-MRI relaxometry. Radiother Oncol 2012; 105: 29-35.

[56] Rimondi E, Benassi MS, Bazzocchi A, Balladelli A, Facchini G, Rossi G, Taieb S, Vanel D. Translational research in diagnosis and management of soft tissue tumours. Cancer Imaging 2016; 16: 1-13.

[57] Tran LB, Bol A, Labar D, Cao-Pham TT, Jordan B, Bregoire V, Gallez B. Predictive value of ^{18}F-FAZA PET imaging for guiding the association of radiotherapy with nimorazole: a preclinical study. Radiother Oncol 2015; 114: 189-194.

[58] Chakravarty R, Goel S, Dash A, Cai W. Radiolabeled inorganic nanoparticles for positron emission tomography imaging of cancer: an overview. Q J Nucl Med Mol Imaging 2017; 61: 181-204.

[59] Welch MJ, Hawker CJ, Wooley KL. The advantages of nanoparticles for PET. J Nucl Med 2009; 50: 1743-6.